JPNT 4(3), 107-114 (2015)
http://dx.doi.org/10.11003/JPNT.2015.4.3.107

JPNT Journal of Positioning, Navigation, and Timing

Pseudo-Correlation-Function Based Unambiguous Tracking Technique for CBOC (6,1,1/11) Signals

Gil-Seop Jeong, Seung-Hyun Kong†
The CCS Graduate School for Green Transportation, KAIST, Daejeon 305-701, Korea

ABSTRACT

Binary Offset Carrier (BOC) signal planned for future Global Navigation Satellite System (GNSS) provided better positioning accuracy and smaller multipath error than GPS C/A signal. However, due to the multiple side peaks in the auto-correlation function (ACF) of the BOC modulated signals, a receiver may false lock onto one of the side peaks in the tracking mode. This false lock would then result in a fatal tracking error. In this paper, we propose an unambiguous tracking method for composite BOC (CBOC) signals to mitigate this problem. It aims to reduce the side peaks of the ACF of CBOC modulated signals. It is based on the combination of traditional CBOC correlation function (CF) and reference CF of unmodulated pseudo- random noise code (PRN code). First, we present that cross-correlation function (CCF) with unmodulated PRN code is close to the secondary peaks of the traditional CBOC. Then, we obtain an unambiguous correlation function by subtracting traditional CBOC ACF from these CFs. Finally, the tracking performance for the CBOC signals is examined, and it is shown that the proposed method has better performance than the traditional unambiguous tracking method in additive white Gaussian noise (AWGN) channel.

Keywords: CBOC signal, pseudo correlation function, unambiguous tracking, side-peak cancellation

1. INTRODUCTION

A Global Navigation Satellite System (GNSS) provides the position, velocity, and time synchronization information of a user through the time of arrival of satellite signals and the ephemeris extracted from the received signals by receiving at least four navigation satellite signals (Borre et al. 2007). Representative GNSS includes the Global Positioning System (GPS) from the United States. In the early stage, GPS was developed for military purposes; but it is currently used in various social and economic fields (e.g., administration and communication) as well as for military purposes since part of the signal (GPS L1 C/A code) has been open to the public. As services based on positioning through a mobile device including vehicle navigation have been actively provided since the 2000s, demand for positioning accuracy that accurately estimates one's own position has continuously increased. Thus, to provide high-quality service by improving the positioning performance and by overcoming the dependence on GPS from the United States, independent GNSS projects have been planned and developed, such as Galileo from the European Union, COMPASS from China, and GLONASS from Russia (Misra & Enge 2006).

Among them, the European Union performed the development of a modernized signal of GNSS in cooperation with the United States in 2004. The modulation technique used for existing GPS L1C is the Binary Phase Shift Keying (BPSK) modulation, where the power spectrum is bilaterally symmetrical as the main lobe is located at the center frequency (1575.42 MHz). The project was the development of a common signal in the GPS L1 band and the Galileo E1 band using this center frequency (1575.42 MHz), and it was

Received July 31, 2015 **Revised** Aug 24, 2015 **Accepted** Aug 26, 2015
†**Corresponding Author**
E-mail: skong@kaist.ac.kr
Tel: +82-42-350-1265 Fax: +82-42-350-1250

designed by separating the main lobe energy by half and by moving it from the center frequency on the power spectrum, considering the compatibility and interoperability with the existing GPS signal. A signal that has been made through this project is the Multiplexed Binary Offset Carrier (MBOC). Among MBOC modulation techniques, the pilot channel of the GPS L1C signal selected the Time-Multiplexed Binary Offset Carrier (TMBOC) technique, and Galileo from the European Union selected the Composite Binary Offset Carrier (CBOC) technique (Avila-Rodriguez et al. 2006, Hein et al. 2006).

A signal that has been examined in this study is the CBOC (6,1,1/11) signal from the European Union. As mentioned earlier, the CBOC signal was designed so that it could efficiently share frequency with the existing GPS signal and the interference could be reduced; and it is capable of more accurate positioning as the distortion of ACF by multipath can be reduced due to a sharper main peak of the auto-correlation function (ACF) compared to that of existing BPSK, which is the advantage of the Binary Offset Carrier (BOC) signal. However, it also has an ambiguity problem due to positive and negative side peaks that BPSK does not have, which is the disadvantage of the BOC signal, besides the sharp main peak of ACF. The ambiguity problem refers to a problem where false lock at the side peaks of ACF occurs during signal tracking and thus the location at which signal tracking is performed cannot be known. It would eventually induce a large positioning error of up to 300m. Therefore, unlike BPSK, an additional technique for eliminating ambiguity is required (Lee et al. 2009).

Representative existing techniques for eliminating ambiguity include BPSK-Like (Martin et al. 2003), bump-jumping (Fine & Wilson 1999), and side-peaks cancellation (Chen et al. 2012). In the BPSK-Like technique, to eliminate the effect of subcarrier that forms side peaks, single sideband auto-correlations are performed in pairs for the signals separated on both sides of a main peak; and based on this, the peak is tracked using ACF that has been formed in a shape similar to that of the ACF of BPSK. In the bump jumping technique, separate tracking channels (very early & very late) are added to both sides of a main peak at spots that are one peak apart from the main peak, and accurate tracking of the peak is determined by comparing the size of the prompt tracking channel and the sizes of the very early & very late tracking channels. Lastly, in the side-peaks cancellation technique which is an innovative technique for resolving ambiguity, a local replica signal with a waveform that is different from that of a received signal is used, and it is mixed with the correlation output result to produce an unambiguous correlation function, which is then used to track the peak. Representative techniques include ASPeCT (Julien et al. 2007) and SCPC (Chen et al. 2012), and most of the mentioned techniques can be applied to a basic BOC signal.

In particular, the ASPeCT technique used a PRN cross-correlation function (CCF) in order to eliminate the side peaks of BOC (n,n). Based on this, in the present study, a new CBOC unambiguous function for the improvement of signal tracking performance was proposed by significantly decreasing side peaks and by partially decreasing the width of a main peak further through the calculation of the ACF of CBOC and the ACF of PRN.

The contents of this paper are as follows. In Chapter 2, a CBOC signal and a correlation function are examined; and in Chapter 3, the ACF and CCF of CBOC and PRN are analyzed and a new unambiguous correlation function is proposed based on this. In Chapter 4, based on simulation, the performance of the proposed unambiguous correlation function is compared with that of an existing technique. Lastly, conclusions are drawn in Chapter 5.

2. SIGNAL MODEL

2.1 Multiplexed Binary Offset Carrier (MBOC) Signal

As mentioned earlier, the MBOC modulated signal was planned as part of the modernization of Galileo and GPS in order to improve the positioning performance at the existing 1575.42 MHz band and to minimize interference with the existing GPS. Before explaining the MBOC modulated signal, the BOC signal, which is a superordinate concept, is explained. The BOC (m,n) signal refers to a signal that has been generated by multiplying PRN spread code and subcarrier and by modulating it into sine wave carrier. Thus, it is defined by two independent variables: the subcarrier frequency, f_{sc} (MHz), and the chip rate of the Pseudorandom Noise code (PRN code), f_c (Mchips/s). m is defined as the ratio of subcarrier frequency, f_{sc}, to reference frequency, (f_0=1.023 MHz), ($m = f_{sc} / f_0$); and n is defined as the ratio of PRN code chip rate, f_c, to reference frequency ($n = f_c / f_0$). For example, BOC (2,1) indicates that it has a subcarrier frequency of 2.046 MHz, and a PRN code chip rate of 1.023 MHz.

MBOC signals are divided into two types: GPS L1C and Galileo E1 OS signals, and they are defined by TMBOC and CBOC, respectively. Basically, the MBOC (m,m',k) signal consists of two components: BOC (m,1) and BOC (m',1), and k represents the power spectrum ratio of BOC (m,1). In general, it is expressed as an MBOC (6,1,1/11) signal, and

http://dx.doi.org/10.11003/JPNT.2015.4.3.107

is generated through the combination of BOC (6,1), which is a wide band, and BOC (1,1), which is a narrow band. A standardized MBOC power spectrum equation that can represent both TMBOC and CBOC is expressed in Eq. (1). In this regard, $G_{BOC(1,1)}$ and $G_{BOC(6,1)}$ represent the power spectra of normalized BOC (1,1) and BOC (6,1), and are expressed in Eq. (2a,b), respectively. Eq. (3) expresses the signal waveform by PRN and data. Lastly, the signal of BOC (m,1) can be expressed as Eq. (4) (Hein et al. 2006, Fantino et al. 2008).

$$G_{MBOC(6,1,1/11)}(f) = \frac{10}{11} G_{BOC(1,1)}(f) + \frac{1}{11} G_{BOC(6,1)}(f) \quad (1)$$

$$G_{BOC(1,1)}(f) = \Im\{S_{BOC(1,1)}(t)\} = \int_{-\infty}^{+\infty} S_{BOC(1,1)}(t) e^{-j2\pi ft} dt \quad (2a)$$

$$G_{BOC(6,1)}(f) = \Im\{S_{BOC(6,1)}(t)\} = \int_{-\infty}^{+\infty} S_{BOC(6,1)}(t) e^{-j2\pi ft} dt \quad (2b)$$

$$S_{PRN}(t) = \sum_{l=-\infty}^{+\infty} c_l \cdot p_{T_c}(t - lT_C) \quad (3)$$

$$S_{BOC(m,1)}(t) = S_{PRN}(t) \cdot \mathrm{sgn}[\sin(2m\pi t / T_C)] \quad (4)$$

where c_l is the l-th PRN code with a value of ±1 and a period of L, and p_{T_c} is the unit size rectangular waveform where the width is the chip spacing, T_c.

Unlike the existing BPSK signal, subcarrier modulation is performed for the BOC signal. This is because the interference can be reduced and the frequency can be shared when the existing BPSK spectrum signal energy concentrated on the center frequency is symmetrically separated based on the center frequency in the case of the BOC modulated signal, and because the positioning accuracy can be improved by forming ACF with a narrower main peak. As a result, the tracking error decreases during signal tracking, which improves the final position accuracy. However, due to side peaks that the BPSK signal does not have, there are multiple false lock points (FLP) in the discriminator output for the BOC signal. FLP refers to a discriminator zero-crossing point where the discriminator output value indicates that it has been synchronized at a proper location but in practice, it has been synchronized at another peak. Fig. 1 shows the discriminator output for BOC (1,1), where four FLPs are observed besides the true lock point (TLP) which is the origin. The ambiguity problem mentioned earlier refers to a problem where it is synchronized at FLP in the signal tracking stage and thus the location at which signal tracking is performed cannot be known (Julien et al. 2004). MBOC also has this problem, similar to the BOC signal. In Chapter 3, ACF for reducing the FLP of CBOC is explained among the MBOCs.

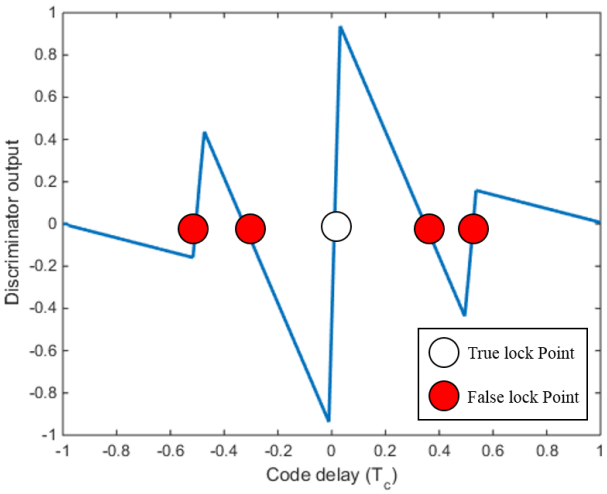

Fig. 1. Discriminator output for BOC (1,1).

2.2 Composite Binary Offset Carrier (CBOC) Signal

For Galileo E1, the CBOC organized by the weighted sum of BOC (6,1) and BOC (1,1) is used as MBOC. In general, it is expressed as *CBOC*(6,1,γ), and γ represents the proportion of the BOC (6,1) power component in the total signal power. The amplitude proportion of BOC (1,1) in the total signal is $\alpha \triangleq \sqrt{1-\gamma}$, and that of BOC(6,1) is $\beta \triangleq \sqrt{\gamma}$. Thus, the signal of CBOC (6,1,1/11) can be expressed as Eq. (5), and the Galileo E1 signal, S_{E1}, can be expressed as Eq. (6).

$$S_{CBOC(6,1,1/11,'+/-')}(t) = \alpha S_{BOC(1,1)}(t) \pm \beta S_{BOC(6,1)}(t) \quad (5)$$

$$\begin{aligned} S_{E1}(t) &= \frac{1}{\sqrt{2}} \begin{bmatrix} e_{E1-B}(t) S_{CBOC(6,1,1/11,'+')}(t) \\ -e_{E1-C}(t) S_{CBOC(6,1,1/11,'-')}(t) \end{bmatrix} \\ &= \frac{1}{\sqrt{2}} \begin{bmatrix} e_{E1-B}(t)(\alpha S_{BOC(1,1)}(t) + \beta S_{BOC(6,1)}(t)) \\ -e_{E1-C}(t)(\alpha S_{BOC(1,1)}(t) - \beta S_{BOC(6,1)}(t)) \end{bmatrix} \end{aligned} \quad (6)$$

The CBOC signal is broadly divided into $\alpha S_{BOC(1,1)}(t) + \beta S_{BOC(6,1)}(t)$ which is a subcarrier function for E1-B for data transmission and $\alpha S_{BOC(1,1)}(t) - \beta S_{BOC(6,1)}(t)$ which is a subcarrier function for pilot E1-C for signal synchronization, and they are expressed as CBOC (6,1,1/11,'+') and CBOC (6,1,1/11,'-'), respectively. In Eq. (5), $e_{E1\text{-}B}$ is the E1-B signal which is generated based on navigation data and PRN code, and $e_{E1\text{-}B}$ is the E1-C signal which is generated based on PRN code as a pilot component. Also, $SC_{(),a}$ is the BOC (1,1) subcarrier component, and $SC_{(),b}$ is the BOC (6,1) subcarrier component. As mentioned earlier, when γ is 1/11, α and β are $\sqrt{\frac{10}{11}}$ and $\sqrt{\frac{1}{11}}$, respectively. Thus, the shape of the signal element is as shown in Fig. 2 (Hein et al. 2006, Avila-Rodriguez et al. 2006).

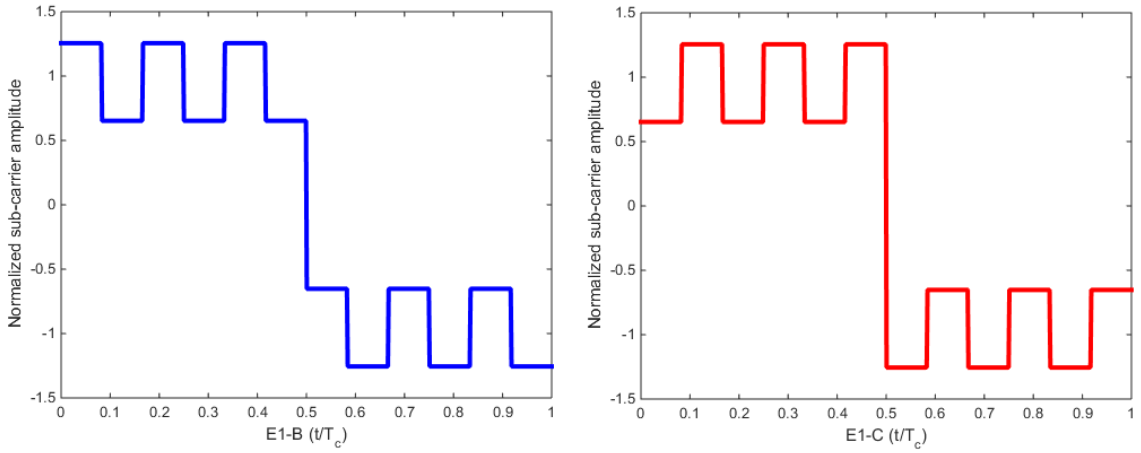

Fig. 2. CBOC subcarrier (E1-B and E1-C).

The ACF of CBOC (6,1,1/11,'+/-') is expressed as Eq. (7a). In this regard, the ACFs of BOC (1,1) and BOC (6,1) can be separately defined as shown in Eq. (7b,c), respectively. T_L is the PRN code period, $k=[2|\tau|]$, and $y=[x]$ is a rounding-up function that outputs the smallest integer y that satisfies $y \geq x$.

$$\begin{aligned} R_{CBOC(6,1,1/11,'+/-')}(\tau) &= \int_0^{T_L} S_{CBOC(6,1,1/11)}(t) S_{CBOC(6,1,1/11)}(t+\tau)dt \\ &= \int_0^{T_L} \left\{ \begin{array}{l} \left[\alpha S_{BOC(1,1)}(t) \pm \beta S_{BOC(6,1)}(t)\right] \times \\ \left[\alpha S_{BOC(1,1)}(t+\tau) \pm \beta S_{BOC(6,1)}(t+\tau)\right] \end{array} \right\} dt \\ &= \int_0^{T_L} \left\{ \begin{array}{l} \alpha^2 S_{BOC(1,1)}(t) S_{BOC(1,1)}(t+\tau) \\ +\beta^2 S_{BOC(6,1)}(t) S_{BOC(6,1)}(t+\tau) \\ \pm\alpha\beta S_{BOC(1,1)}(t) S_{BOC(6,1)}(t+\tau) \\ \pm\alpha\beta S_{BOC(6,1)}(t) S_{BOC(1,1)}(t+\tau) \end{array} \right\} dt \\ &= \alpha^2 R_{BOC(1,1)}(\tau) + \beta^2 R_{BOC(6,1)}(\tau) \pm 2\alpha\beta R_{BOC(1,1)} R_{BOC(6,1)}(\tau) \end{aligned} \quad (7a)$$

$$R_{BOC(1,1)}(\tau) = \begin{cases} 1-3|\tau|, & |\tau| \leq \frac{1}{2}T_c \\ -1+|\tau|, & \frac{1}{2}T_c < |\tau| \leq T_c \\ 0, & \text{otherwise} \end{cases} \quad (7b)$$

$$R_{BOC(6,1)}(\tau) = \begin{cases} (-1)^{k+1}[\alpha - \beta|\tau|], & |\tau| \leq T_c \\ 0, & \text{otherw} \end{cases} \quad (7c)$$

Fig. 3 shows the ACF of CBOC (6,1,1/11,'+/-') along with those of BPSK, BOC (1,1), and BOC (6,1). The ACFs of the BOC (1,1) and CBOC signals had similar shapes, but the CBOC ACF had a sharper main peak than BOC (1,1). It is due to the BOC (6,1) component which is a high-frequency component in CBOC, and more precise positioning is enabled based on this. However, similar to the existing BOC signal, CBOC also has side peaks, and this causes an ambiguity problem. Therefore, an additional

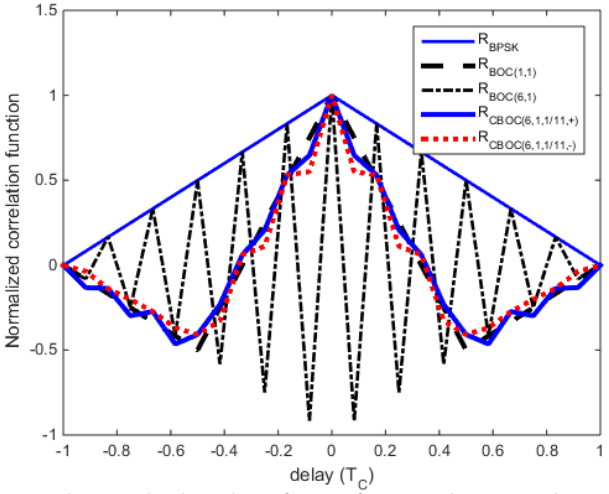

Fig. 3. The normalized correlation function for BOC and CBOC signal.

synchronization technique is required. Thus, in the next chapter, an unambiguous correlation function that can increase precision by significantly decreasing side peaks and by making a sharper main peak based on the side-peak cancellation technique is introduced.

3. PROPSED UNAMBIGUOUS AUTOCORRELATION FUNCTION

Among the representative techniques for resolving an ambiguity problem (BPSK-Like, bump-jumping, and side-peaks cancellation), the technique proposed in the present study is a kind of side-peaks cancellation technique which makes new ACF by eliminating or minimizing the ACF side peaks of an existing signal through generating a local signal during the tracking of a CBOC signal.

The proposed technique generates ACF with a local

signal that consists only of PRN code as well as a local signal such as transmission CBOC for tracking an existing CBOC signal. The ACF of existing CBOC basically has large negative side peaks on both sides of a main peak. This characteristic is well represented in Fig. 4, which shows the ACF of existing CBOC, the unambiguous correlation function of CBOC proposed in the present study, the absolute value of CBOC-PRN CCF using PRN for explaining this, and the absolute value of existing CBOC ACF. To eliminate these side peaks, the Julien technique using a PRN cross-correlation function (Julien et al. 2007) was applied in the present study. As shown in Fig. 4, for the absolute value of the ACF between the CBOC signal and the local PRN signal, $|R_{CBOC\text{-}PRN}|$, the trend of the peaks on both sides is similar to that of the absolute value of the ACF of the existing CBOC, $|R_{CBOC(6,1,1/11,-)}|$. Thus, an unambiguous correlation function was generated using the difference between the $|R_{CBOC(6,1,1/11,-)}|$ and the $|R_{CBOC\text{-}PRN}|$, which is the absolute value of the ACF with the local PRN signal.

The PRN code sequence used in $|R_{CBOC\text{-}PRN}|$ was assumed to be the PRN sequence used in E1-C (i.e., pilot channel) for signal tracking as shown in Eq. (3), and the auto-correlation function with the CBOC signal is expressed in Eq. (8). In this regard, $tri_{\alpha}\left(\frac{x}{y}\right)$ is a function of x with a width of y centering on α. Using this, to eliminate side peaks from the absolute value of the ACF of existing CBOC, an unambiguous correlation function was proposed in the present study based on the difference from the absolute value of $|R_{CBOC\text{-}PRN}|$. It is expressed as shown in Eq. (9).

$$R_{CBOC/PRN}(\tau)=\int_0^{T_L} S_{CBOC(6,1,1/11,'-')}(t)S_{PRN}(t+\tau)dt = \frac{1}{2}\left(tri_{-\frac{1}{2}}\left(\frac{\tau}{T_c}\right)-tri_{\frac{1}{2}}\left(\frac{\tau}{T_c}\right)\right) \quad (8)$$

$$R_{Proposed}(\tau)=|R_{CBOC}(\tau)|^2-|R_{CBOC-PRN}(\tau)|^2 \quad (9)$$

As shown in Fig. 4, the proposed unambiguous correlation function, $R_{Proposed}$, has significantly smaller side peaks than the existing CBOC ACF R_{CBOC}, and has a sharper main peak than the existing correlation function. Therefore, it is expected that the signal tracking performance would be improved due to the sharp main peak, and that ambiguity where it is synchronized at side peaks could be reduced.

In addition, the discriminator output for CBOC signal tracking can be expressed as shown in Fig. 5. The discriminator used in this study was a noncoherent early minus late power (NELP) discriminator. When compared to the ACF of the existing CBOC, FLP where a discriminator crosses zero points due to side peaks disappeared, and the slope of the linear section with TLP became larger. Thus, improvement in the signal tracking performance is expected in the same noise environment.

The final output value through the discriminator is expressed in Eq. (13), and the early-late discrimination values of the I and Q channels, I_E, I_L, Q_E, and Q_L, are expressed in Eq. (12), respectively. In this regard, when D is the navigation data, Δ is the early-late spacing (with $\Delta \le T_c$), $X(t)$ is the spread sequence, $\tilde{X}(t)=X(t)*h(t)$ is the filtered spread sequence, and $h(t)$ is the impulse response of the receiver input filter, the raised cosine filter can be defined as Eq. (10), where B_W is the filter bandwidth and ξ is the roll-off factor ($0\le\xi\le1$). Also, the cross-correlation function of $X(t)$ and $\tilde{X}(t)$ is expressed in Eq. (11) (Van Dierendonck et al. 1992).

$$h(t)=\mathrm{sinc}(2B_W t)\left[\frac{\cos(2\pi\xi B_W t)}{1-16\xi^2 B_W^2 t^2}\right] \quad (10)$$

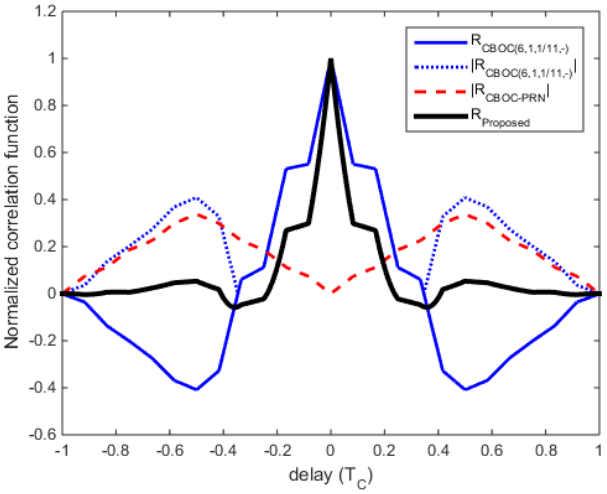

Fig. 4. The normalized correlation function for CBOC.

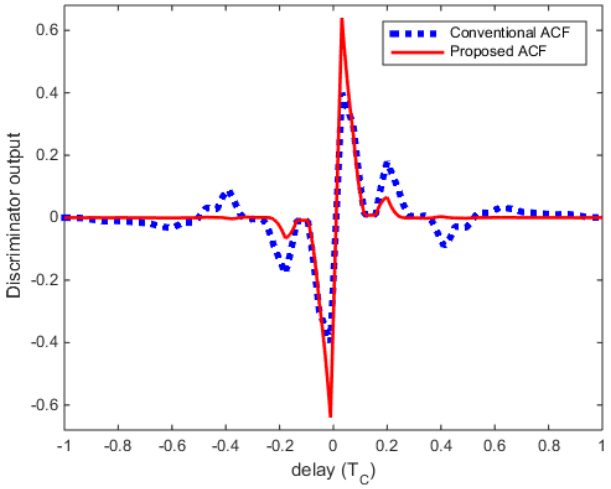

Fig. 5. Discriminator outputs of correlation functions.

$$R_{\tilde{X}X}(\tau)=\int_0^{T_L} X(\tau)X(t-\tau)dt=R_X(\tau)*\mathrm{h}(\tau) \quad (11)$$

$$I_E(\tau)=ADR_{\tilde{X}X}\left(\tau-\frac{\Delta}{2}\right)\mathrm{sin}\,c(f_eT)\cos(\pi f_eT+\theta_e)+N_{i,E}$$

$$I_L(\tau)=ADR_{\tilde{X}X}\left(\tau+\frac{\Delta}{2}\right)\mathrm{sinc}(f_eT)\cos(\pi f_eT+\theta_e)+N_{\mathrm{i,L}}$$

$$Q_E(\tau)=ADR_{\tilde{X}X}\left(\tau-\frac{\Delta}{2}\right)\mathrm{sinc}(f_eT)\sin(\pi f_eT+\theta_e)+N_{\mathrm{q},E}$$

$$Q_L(\tau)=ADR_{\tilde{X}X}\left(\tau+\frac{\Delta}{2}\right)\mathrm{sinc}(f_eT)\sin(\pi f_eT+\theta_e)+N_{\mathrm{q,L}} \quad (12)$$

$$d(\tau)=\frac{[(I_E^2(\tau)+Q_E^2(\tau))-(I_L^2(\tau)+Q_L^2(\tau))]}{2} \quad (13)$$

where f_e is the frequency error; θ_e is the phase error; $N_{i,E}$, $N_{i,\mathrm{L}}$, $N_{\mathrm{q},E}$, and $N_{\mathrm{q,L}}$ are the noise components included in the early and late components of the I and Q channels; and A is the amplitude of the signal.

The discriminator operates until the output of the discriminator, $d(\tau)$, becomes 0, by the numerically controlled oscillator within the delayed lock loop (DLL). Eventually, through the calculation of the cross-correlation function between the BOC signal and the unmodulated PRN code, $R_{CBOC\text{-}PRN}$, during signal tracking, the possibility of false lock at the side peaks can be significantly decreased by significantly reducing the side peaks; the slope of the linear section of the discriminator increases by partially decreasing the width of the main peak further; and the signal tracking performance is improved by eliminating the FLP.

4. SIMULATION

The performance of the unambiguous correlation function proposed in this study was evaluated and compared with that of the existing technique through tracking error standard deviation (TESD) and multipath error envelope (MEE) simulations for signal tracking. Table 1 summarizes the simulation parameters. B_L is the loop filter bandwidth; T_I is the integration time; Δ is the chip width used for the narrow correlator, which represents the interval between early and late; and T_C^{-1} is the PRN code speed.

TESD is defined as $\frac{\sigma}{G}\sqrt{2B_LT_I}$, where σ is the standard deviation of $D(\tau)|_{\tau=0}$; $G=\frac{dD(\tau)}{d\tau}|_{\tau=0}$ represents the slope when the delay of the discriminator, τ, is 0; B_L is the loop filter bandwidth; and T_I is the integration time (Lee et al. 2009).

Fig. 6 shows the tracking error standard deviation for the CBOC signal depending on the carrier-to-noise ratio (CNR) when the existing correlation function and the proposed correlation function were used, respectively. In this regard, CNR is defined as P/N_0, and N_0 is the noise power density. The CNR region of interest was 20 ~ 50 [dB-Hz], and the proposed correlation function showed a better tracking error standard deviation than the existing correlation function.

Figs. 7-9 show the multipath error envelope outputted by changing the multipath delay using the line of sight (LOS) signal and the multipath signals that have decreased by $\alpha(0\le\alpha\le1)$ times compared to the LOS signal due to multipath and that have been delayed by τ as shown in Eq. (14).

$$r(t)=AX(t)\cos[(\omega_0+\omega_d)t+\theta_0]+\sum_{n=1}^{N}\alpha_nAX(t-\tau_n)\cos[(\omega_0+\omega_d)t+\theta_0+\phi_n]+n(t) \quad (14)$$

where w_0 is the basic frequency component, w_d is the frequency offset component due to Doppler and oscillator, $\mathrm{R}_{\tilde{X}X}$ is the cross-correlation function between the filtered code sequence and the code sequence of the received signal, and τ_n and ϕ_n are the delay time and phase change components of the n-th NLOS signal component, respectively. The NELP correlator output is expressed in Eq. (15).

$$\begin{aligned}
I_E(\varepsilon)&=AD\,\mathrm{sin}\,c(f_eT)\left\{R_{\tilde{X}X}\left(\varepsilon-\frac{\Delta}{2}\right)\cos(\pi f_eT+\theta_e)+\sum_{n=1}^{N}\alpha_n\mathrm{R}_{\tilde{X}X}\left(\varepsilon-\frac{\Delta}{2}-\tau_n\right)\cos(\pi f_eT+\theta_e+\phi_n)\right\}+N_{i,E}\\
I_L(\varepsilon)&=AD\,\mathrm{sin}\,c(f_eT)\left\{R_{\tilde{X}X}\left(\varepsilon+\frac{\Delta}{2}\right)\cos(\pi f_eT+\theta_e)+\sum_{n=1}^{N}\alpha_n\mathrm{R}_{\tilde{X}X}\left(\varepsilon+\frac{\Delta}{2}-\tau_n\right)\cos(\pi f_eT+\theta_e+\phi_n)\right\}+N_{i,L}\\
Q_E(\varepsilon)&=AD\,\mathrm{sin}\,c(f_eT)\left\{R_{\tilde{X}X}\left(\varepsilon-\frac{\Delta}{2}\right)\sin(\pi f_eT+\theta_e)+\sum_{n=1}^{N}\alpha_n\mathrm{R}_{\tilde{X}X}\left(\varepsilon-\frac{\Delta}{2}-\tau_n\right)\sin(\pi f_eT+\theta_e+\phi_n)\right\}+N_{q,E}\\
Q_L(\varepsilon)&=AD\,\mathrm{sin}\,c(f_eT)\left\{R_{\tilde{X}X}\left(\varepsilon+\frac{\Delta}{2}\right)\sin(\pi f_eT+\theta_e)+\sum_{n=1}^{N}\alpha_n\mathrm{R}_{\tilde{X}X}\left(\varepsilon+\frac{\Delta}{2}-\tau_n\right)\sin(\pi f_eT+\theta_e+\phi_n)\right\}+N_{q,L}
\end{aligned} \quad (15)$$

Table 1. Simulation environment.

Parameter	Value
B_L	10 Hz
T_I	1 ms
Δ	1/24 [T_C]
T_C^{-1}	1.023 MHz

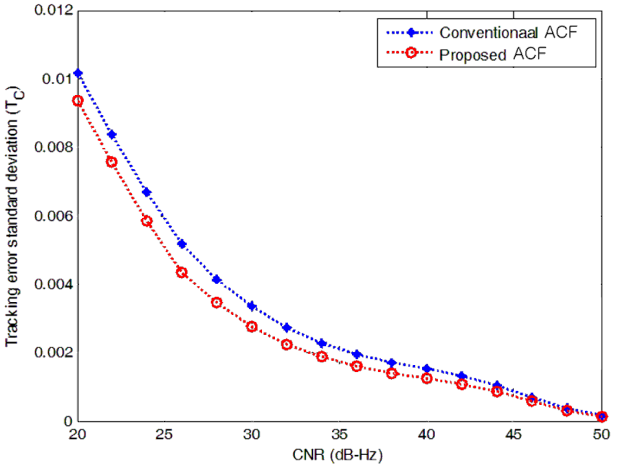

Fig. 6. Tracking error standard deviation (TESD).

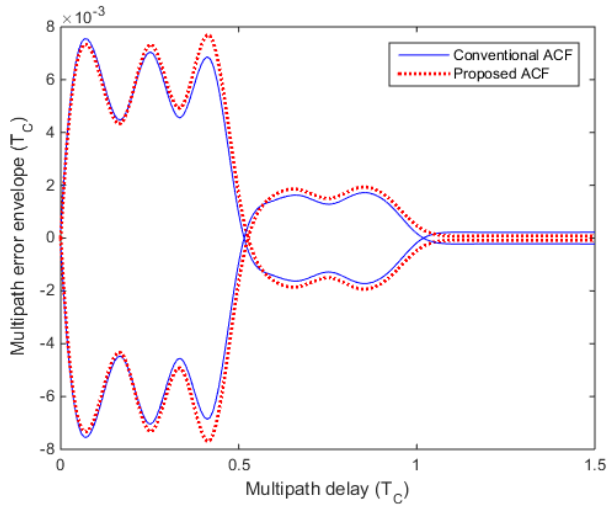

Fig. 7. Multipath error envelop ($N=1$).

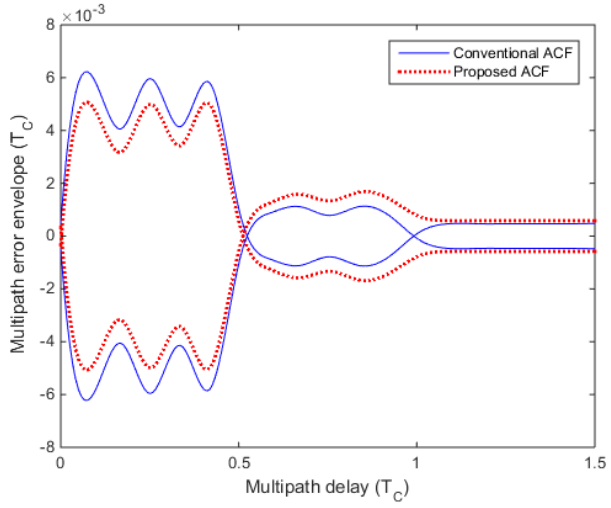

Fig. 8. Multipath error envelop ($N=2$).

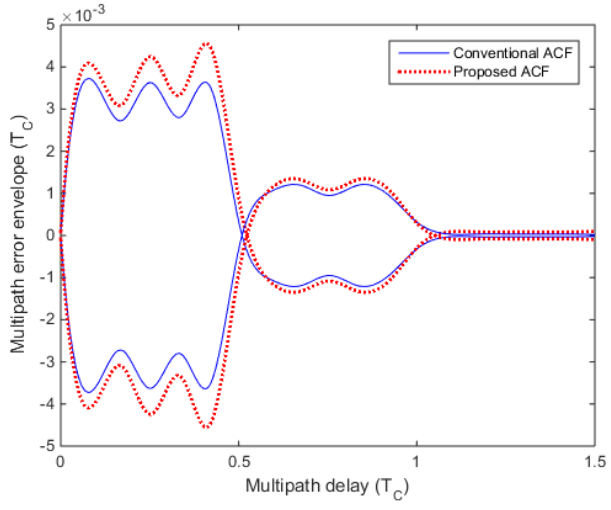

Fig. 9. Multipath error envelop ($N=3$).

For the simulation shown in Fig. 7, [N=1, α_1=0.5, ϕ_1=0,π] was used, and the performance was similar to that of the existing technique. In addition, simulations were performed by increasing the multipath component using the following parameters when N=2 and N=3, as shown in Figs. 8 and 9, respectively, In the case of N=2, [α_1=0.2, ϕ_1=0,α_2, ϕ_2=π, τ_2=0.5T_c] and [α_1=0.2, ϕ_1=π, α_2=0.5, ϕ_2=0, τ_2=0.5T_c] were used; and in the case of N=3, [α_1=0.3, ϕ_1=0.3, ϕ_2=0, τ_2=0.3T_c, α_3=0.5, ϕ_3=0, τ_3=0.7T_c] and [α_1=0.3, ϕ_1=π, α_2=0.3, ϕ_2=π, τ_2=0.3T_c, α_3=0.5, ϕ_3=π, τ_3=0.7T_c] were used. As a result, there was a case where the performance was improved compared to that of the existing technique, but there also were cases where the performance deteriorated or the performance was similar. Considering the main peak characteristics of the ACF of the proposed technique, it was expected that the resolution would be superior due to the narrow ACF main peak of the multipath. However, it is thought that the performances shown in Figs. 7-9 were observed because the model of the received signal is based on the nonlinear combination of the convolution term of $R_{CBOC}(\tau)$ and channel and the convolution term of $R_{CBOC\text{-}PRN}(\tau)$ and channel, rather than the convolution form of $R_{Proposed}(\tau)$ and channel, as shown in Eq. (9). Also, it is thought that the proposed technique is more robust to the effect of noise, rather than performance improvement relevant to multipath.

5. CONCLUSIONS

In this study, an unambiguous correlation function using a pseudo correlation function was proposed for the tracking of CBOC signals. Based on the fact that the side peak of CBOC ACF and the CCF of a pseudo correlation function show similar trends, the height of the side peak was significantly decreased using the difference between the values obtained by taking an absolute value. The result of the tracking error standard deviation simulation showed that the proposed unambiguous correlation function had superior signal tracking performance in various CNR environments compared to the existing technique, and the result of the multipath error envelope simulation showed that the performances were similar in terms of multipath delay. Therefore, studies on the robustness to multipath delay are needed in the future based on the additional supplementation of the unambiguous function.

ACKNOWLEDGMENTS

This research (2013R1A2A2A01067863) was supported by

Mid-career Researcher Program through NRF grant funded by the Korean government (MEST).

REFERENCES

Avila-Rodriguez, J. A., Wallner, S., Hein, G., Rebeyrol, E., Julien, O., et al. 2006, CBOC – An Implementation of MBOC. In CNES-ESA, 1st Workshop on GALILEO signals and Signal Processing.

Borre, K., Akos, D. M., Bertelsen, N., Rinder, P., & Jensen, S. H. 2007, A Software-Defined GPS and Galileo Receiver: A Single-Frequency Approach (Boston: Birkhäuser), pp.69-73. http://dx.doi.org/10.1007/978-0-8176-4540-3

Chen, H. H., Ren, J. W., & Yao, M. L. 2012, Side-peak cancellation general framework designed for BOC signals unambiguous processing, Journal of Astronautics, 33, 1646-1653.

Fantino, M., Marucco, G., Mulassano, P., & pini, M. 2008, Performance analysis of MBOC, AltBOC, and BOC modulations in terms of multipath effects on the carrier tracking loop within GNSS receivers, in Proc. IEEE/ION PLANS, Monterey, CA, pp.369-376. http://dx.doi.org/10.1109/PLANS.2008.4570092

Fine, P. & Wilson, W. 1999, Tracking algorithm for GPS offset carrier signals. Proceedings of the 1999 National Technical Meeting of The Institute of Navigation, pp. 671-676.

Hein, G. W., Avila-Rodriguez, J. A., Wallner, S., Pratt, A. R., Owen, J., et al. 2006, MBOC: The new optimized spreading modulation recommended for Galileo L1 OS and GPS L1C, Proceedings of IEEE/ION PLANS, San Diego, CA, pp.883-892. http://dx.doi.org/10.1109/PLANS.2006.1650688

Julien, O., Cannon, M. E., Lachapelle, G., Mongredien, C., & Macabiau, C. 2004, A new unambiguous BOC (n,n) signal tracking technique, Proceeding of the GNSS 2004 Conf., Rotterdam, The Netherlans, May 17-19.

Julien, O., Macabiau, C., Cannon, M. E., & Lachapelle, G. E. 2007, ASPeCT: Unambiguous sine-BOC (n,n) acquisition/tracking technique for navigation application, IEEE Transactions on Aerospace and Electronic Systems, 43, 150-162. http://dx.doi.org/10.1109/TAES.2007.357123

Lee, Y., Yoon, T., Lee, M., Lee, Y., Kim, S., et al. 2009, A new CBOC correlation function for next generation GNSS signal synchronization, J. Korean Inst. Commun. Sci. (KICS), 34, 724-729.

Martin, N., Leblond, V., Guillotel, G., & Heiries, V. 2003, BOC (x, y) signal acquisition techniques and performances, Proceedings of the 16th International Technical Meeting of the Satellite Division of The Institute of Navigation, ION GPS/GNSS 2003, pp.188-198. http://www.ion.org/publications/abstract.cfm?articleID=5194

Misra, P. & Enge, P. 2006, Global Positioning System: Signals, Measurements, and Performance, Second Edition (Lincoln, MA: Ganga-Jamuna Press)

Van Dierendonck, A. J., Fenton, P., & Ford, T. 1992, Theory and performance of narrow correlator spacing in a GPS receiver, NAVIGATION: Journal of the Insititute of Navigation, 39, 265-283. http://dx.doi.org/10.1002/j.2161-4296.1992.tb02276.x

Gil-Seop Jeong received the B.S degree in Electrical Engineering from Ajou University, Korea, in 2014. From 2014, he is studying form master's degree at the CCS Graduate School for Green Transportation in the Korea Advanced Institute of Science and Technology (KAIST). His research interests include next generation GNSS, advanced signal processing for navigation system.

Seung-Hyun Kong received the B.S. degree in Electronics Engineering from the Sogang University, Korea, in 1992, the M.S. degree in Electrical Engineering from the Polytechnic University, New York, in 1994, and the Ph.D. degree in Aeronautics and Astronautics from Stanford University, CA, in 2006. From 1997 to 2004, he was with Samsung Electronics Inc. and Nexpilot Inc., both in Korea, where his research focus was on wireless communication systems and UMTS mobile positioning technologies. In 2006 and from 2007 to 2009, he was a staff engineer at Polaris Wireless Inc., Santa Clara, and at the Corporate R&D of Qualcomm Inc., San Diego, respectively, where his research was on Assisted-GNSS and wireless positioning technologies such as wireless location signature and mobile-to-mobile positioning technologies. Since 2010, he is with the Korea Advanced Institute of Science and Technology (KAIST), where he is currently an associate professor at the CCS graduate school for green transportation. His research interests include next generation GNSS, advanced signal processing for navigation systems, and vehicular communication systems.